vegetative barriers on surface runoff velocity

Journal of Ecological Engineering, 2026, 27(1), 365–379 https://doi.org/10.12911/22998993/210377 ISSN 2299–8993, License CC-BY 4.0

Impact of *Miscanthus giganteus* and short-rotation coppice

Abdeljalil Boutarfa^{1,2*}, Tarik Benabdelouahab³, Rachid Aboutayeb², Manssens Gilles⁴, Gilles Swerts¹, Yves Brostaux¹, Charles Bielders⁵, Degré Aurore¹

- ¹ Gembloux Agro-Bio Tech, Université de Liège, Passage des Deportes 2, BE-5030 Gembloux, Belgium
- ² Soil, Plant and Water Laboratory, Regional Center of Agricultural Research of Settat, National Institute of Agricultural Research, Avenue Ennasr, BP 415 Rabat Principale, Rabat 10090, Morocco
- ³ Department of Environment and Natural Resources, National Institute of Agricultural Research, Avenue Ennasr, BP 415 Rabat Principale, Rabat 10090, Morocco
- ⁴ CIPF, AgroLouvain-Services, Université catholique de Louvain, Chemin du Cyclotron 2, L7.05.11, BE-1348 Louvain-la-Neuve, Belgium
- ⁵ Earth and Life Institute, Environmental Sciences, Université catholique de Louvain, Croix du Sud 2, L7.05.02, BE-1348 Louvain-la-Neuve, Belgium
- * Correspodning author's e-mail: abdeljalil.boutarfa@uliege.be

ABSTRACT

Accelerated erosion can have detrimental effects on the chemical, physical, and biological quality of soils and surface water bodies. It impacts agricultural productivity and soil ecosystem services. Vegetative barriers can help address this challenge by regulating flows within agricultural watersheds, reducing runoff velocity, and trapping eroded sediments. However, only a limited number of documented studies have quantified the effectiveness of Miscanthus giganteus and short rotation coppie (SRC) against surface runoff. Therefore, this study specifically aims to investigate the effectiveness of these two vegetative barriers in reducing surface runoff and facilitating infiltration. A series of runoff simulation experiments were conducted on silt loam soils in Wallonia (Belgium) between 2021 and 2024, focusing on Miscanthus giganteus and SRC willow strips with varying planting densities and ages (2 to 12 years) on slopes ranging from 4 to 12%. This allowed to determine the hydraulic roughness based on the water depth in the vegetation strip. The runoff simulation results reveal a Manning coefficient (n) ranging between 0.37 and 0.8 s.m^{-1/3} for Miscanthus giganteus and between 0.32 and 0.59 s.m^{-1/3} for SRC depending on different factors (slope, plant density, flow rate and age of plantation). These findings suggest that vegetation strips, particularly Miscanthus giganteus, may be more effective than conventionally used grass strips in slowing down surface flows. Moreover, measurements using the water balances of the runoff tests indicate an infiltration rate of 130±30 mm/h for SRC and 83±20 mm/h for Miscanthus giganteus, showcasing the ability of both barriers to absorb upland runoff. Overall, these results underscore the potential of Miscanthus giganteus and SRC willow strips to improve hydrological functioning of agricultural catchments.

Keywords: Miscanthus giganteus, short rotation coppice, erosion, infiltration, hydraulic roughness.

INTRODUCTION

Preserving natural resources, including soil, is crucial for maintaining sustainable agriculture (Aboutayeb et al., 2020). Soil erosion has become a significant environmental issue, especially on agricultural lands (Pimentel et al., 1995). Soil erosion by water occurs when water, unable to infiltrate the soil, runs off over the land, carrying

away soil particles (Le Bissonnais et al., 2002). In Europe, especially where loamy soils are cultivated with annual crops (Kervroëdan et al., 2018), the occurrence of intense runoff and soil erosion is a common issue (Gobin et al., 2003). Furthermore, climate change, potentially affecting the quantity, timing, and spatial distribution of precipitation, may contribute to the acceleration of soil erosion (Rodrigues et al., 2021). Addressing

Received: 2025.07.25 Accepted: 2025.09.06

Published: 2025.11.25

and mitigating these issues is crucial for sustaining agricultural productivity, preserving soil health, and preventing the broader environmental consequences associated with soil erosion.

Soil loss is intricately linked to precipitation, primarily resulting from the erosive impact of raindrops on the soil surface and the force generated by runoff water (Salles et al., 2000). These forces can be effectively mitigated through intra-plot management practices, which encompass soil conservation practices, crop rotations and the maintenance of permanent vegetation cover. In addition, interplot methods (at field boundaries) such as vegetative barriers and optimized parcel fragmentation, can be employed to reduce runoff connectivity and sediment transport (Herpoel et al., 2025).

A particularly effective method for erosion control is the establishment of vegetative strips along the lower edges of erosion-prone fields. These strips can vary in width, species composition, and plant density, depending on site conditions and management goals. Due to their cost-effectiveness, high efficiency, and environmentally friendly nature, vegetative strips are widely used in ecological soil management (Zhao et al., 2023). In addition to reducing erosion, they enhance biodiversity and contribute to the aesthetic value of agricultural landscapes (Richet et al., 2017).

The presence of vegetation helps mitigate erosion by reducing the kinetic energy of rainfall and providing ground cover (Zhao et al., 2023). Plant roots stabilize the soil (Gyssels et al., 2005) and improve its physical properties, including shear strength and aggregate stability(Gao et al., 2009). Additionally, biochemical interactions between plant roots and the soil enhance soil cohesion and increase organic matter content, further strengthening the soil's resistance to erosion (Xiong et al., 2018; Zhao et al., 2023). Vegetation strips also slow runoff by increasing surface roughness through plant stems and leaves, which in turn enhances sediment deposition (Yuan et al., 2009; Zhang et al., 2015).

Historically, most research regarding vegetative strips has dealt with grassy vegetation. Although grass buffer strips may have multiple functions, their economic value is generally limited. Hence, there is a rising interest in the use of vegetative strips composed of biomass crops, such as *Miscanthus giganteus* or poplar short-rotation coppice (SRC). These crops possess vegetation, either herbaceous or woody, with economic value

and whose characteristics may also be of interest for the mitigation of soil erosion.

Miscanthus giganteus (Figure 1), a sterile hybrid bioenergy crop (Heaton et al., 2008), takes 3 to 5 years to establish and remains productive for up to 25 years (Zub and Brancourt-Hulmel, 2010). It enhances soil resistance to erosion by reducing surface runoff (Zhao et al., 2023) and improving soil aggregate stability (Evers et al., 2013). In recent years, Miscanthus giganteus has gained prominence as a biomass crop(Lewin et al., 2023). It is typically planted from rhizomes at a density of around 15,000 plants per hectare, with spacing of 0.75 to 1 meter. Unlike continuous vegetation cover, Miscanthus giganteus forms clusters of stems from rhizomes, with a natural mulch layer developing between patches as leaves fall and decompose over winter. This mulch plays a crucial role in limiting runoff (Van Dijk et al., 1996) by reducing direct soil exposure to raindrop impact, and enhancing infiltration. Miscanthus giganteus typically grows to 2.5–4 meters in height, with 20–30 stems per plant, a high leaf area index (LAI), and deep rhizome systems extending to 1.5-2 meters (Urrego et al., 2021).

Short-rotation coppice (Figure 1) represents an intensive cultivation method in which poplar or willow stems are planted at high densities, ranging from 12000 to 20000 plants per hectare. SRC is recognized for their large biomass production and positive effects on soil physical quality of the topsoil (Kahle and Janssen, 2020). Their vegetation structure including LAI values of 3–6, stem heights of 3–6 meters, and high stem density enhances surface roughness, reduces runoff velocity, and promotes infiltration. A key component of SRC systems is the herbaceous undergrowth, which further increases roughness, limits soil detachment, and contributes to soil reinforcement by roots (Eppler and Petersen, 2007)

The efficiency of vegetative barriers in reducing runoff and enhancing infiltration has been widely demonstrated (Table 1). Numerous studies have confirmed the effectiveness of grass strips (Bissonnais et al., 2004.; Pan et al., 2017), herbaceous hedges (Blanco-Canqui et al., 2004; Dabney et al., 2012), fascines (Frankl et al., 2021; Richet et al., 2017), and woody hedges (Freeman et al., 2000; Wallace et al., 2021) in controlling erosion. However, the potential of *Miscanthus giganteus* and SRC for this purpose remains underexplored.





Figure 1. Illustration of short rotation coppice barriers (a) and Miscanthus giganteus barriers (b)

In Saunier et al. (2018), a Manning coefficient of 0.62 m·s^{-1/3} was identified for *Miscanthus giganteus*, and 0.4 s.m^{-1/3} for short-rotation coppice, with an infiltration rate of 100 mm/h and 94 mm/h for *Miscanthus giganteus* and short-rotation coppice in a loamy soil, respectively. However, the effectiveness of vegetative barriers such as *Miscanthus giganteus* and short-rotation coppice (SRC) in mitigating runoff and erosion is influenced by various environmental and management factors.

Richet et al. (2014) found that preferential flow pathways reduced the Manning coefficient by 50% when these pathways accounted for 20–25% of the patch area, while Van Dijk et al., (1996) demonstrated that removing mulch from *Miscanthus giganteus* barriers significantly decreased their hydraulic roughness, reducing the Manning coefficient from 0.63 to 0.3 s·m^{-1/3}, emphasizing the importance of maintaining ground cover.

Despite these insights, the specific impact of slope gradient on the effectiveness of *Miscanthus giganteus* barriers remains poorly documented. Research on the influence of plant age on runoff reduction is also limited, though some sources suggest that *Miscanthus giganteus* reaches significant effectiveness by its second year after planting; further investigation is needed to clarify how plant age interacts with slope gradient to affect runoff mitigation. Additionally, while

planting density shapes vegetation structure, its direct role in controlling runoff remains insufficiently explored.

This study aims to fill these knowledge gaps by evaluating the performance of *Miscanthus giganteus* and SRC barriers under diverse site conditions, identifying the key factors that drive their effectiveness, and developing a predictive model to optimize their design and management for improved runoff control.

MATERIALS AND METHODS

Study sites

The study was carried out at 8 sites, with six sites dedicated to *Miscanthus giganteus* barriers and two to SRC barriers, One of the two SRC sites (Eghezée) was used for two consecutive years. These experimental sites are situated in Wallonia (Figure 2), the southern half of Belgium. Notably, the sites differ in terms of slope gradient and the age of plantation (Table 2). However, soil texture was similar at all sites (silt loam soil). Additionally, all *Miscanthus giganteus* sites under study feature mulch, while the SRC sites feature a grass cover. The vegetative barriers are oriented perpendicular to the slope for optimal effectiveness.

Table 1. Effectiveness of some vegetative barriers against soil erosion

Daramatar	Efficiency against soil erosion				
Parameter	Infiltration capacity (mm/h)	Manning coefficient (s.m ^{-1/3})	Sedimentation (%)		
Grass strips	23 to 575 (Souiller et al., 2002)	0.2 to 0.4 (Saunier et al., 2018)	75.8 to 99 (Van Dijk et al., 1996)		
Fascines	35 ± 50 (Richet et al., 2017)	0.4 to 3.0 (Ouvry et al., 2012; Richet et al., 2017)	32 to 73 (Ouvry et al., 2012)		
Shrub hedges	400 ± 100 (Richet et al. 2017)	0.06 to 0.8 (Ouvry et al., 2012; Richet et al. 2017)	31 to 69 (Ouvry et al., 2012)		
Grass hedges	135 to 211 (Rachman et al., 2004)	0.19 to 1.24 (Richet et al., 2019)	69 to 87 (Richet et al., 2019)		

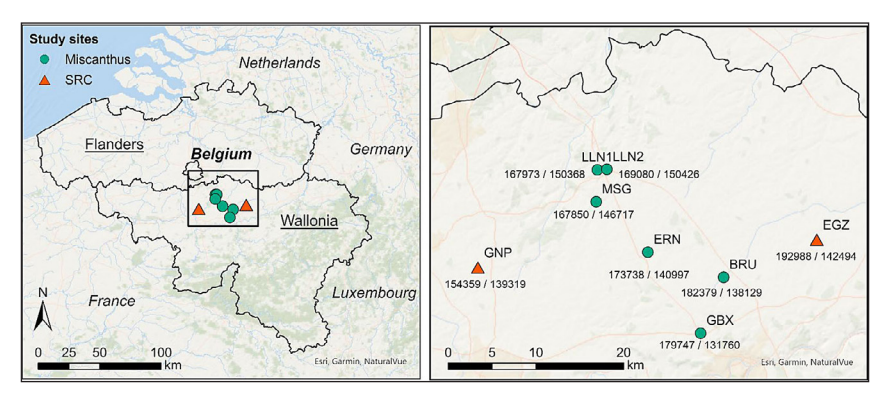


Figure 2. Location of experimental sites (abbreviations are described in Table 2)

Runoff simulation

A runoff simulator (Figure 3) was employed to conduct runoff tests. It generates controlled runoff with a known flow rate within a plot of precisely defined dimensions. It allows precise monitoring of inflow and outflow discharges. The primary component of the simulator is a sloped metal slide, adjustable to a length of 2 meters and with a width of 1 meter. This slide directs water into the natural surface under investigation. A network of pumps connected to a reservoir ensures a constant and controlled discharge. Both the upstream and downstream discharge are monitored using flow meters. The entire system is powered by a nearby electricity source or a generator.

Experimental protocol

At the *Miscanthus giganteus* experimental sites, a total of 14 plots were investigated across the 6 sites, each characterized by varying slopes, ages and stem densities (Table 2). Similarly, for the SRC experimental sites, 6 plots were considered across the two tested sites, each plot exhibiting different observed ages and plant densities (Table 2). The dimensions of each plot were standardized to 3 meters in length and 1 meter in width. This experimental setup follows a protocol akin to the one employed by (Saunier et al., 2018).

To evaluate the efficiency of each vegetative barrier in reducing runoff, water heights across the barrier were measured once the inflow and outflow flow rates reached a steady state. A total of 16 measurements (Figure 4) were taken at each plot. The measurement protocol involved four readings of the water level along the length of the barrier. The first measurement was performed at the beginning of the barrier

(0.2 m from the upstream edge of the vegetation strip), followed by measurements taken at one meter, two meters, and 2.7 meter from the upstream edge of the vegetation strip. At each measurement position, four colored sticks (Figure 5) were positioned across the barrier's width, serving as markers for the measurement points. Flow rates from 0.5 to 4 l/s were selected for our study. The flow rate range is grounded in the investigations conducted in 2018 in Seine-Maritime by Saunier et al. (2018). Beyond the opportunity for comparison with the previous studies, the determination of this range was influenced by practical considerations, with the available pump capacity restricting the feasible flow rates.

Quantifying the effectiveness of the vegetative barriers in limiting the runoff

Several indicators have been used to assess the efficiency of vegetative structures in reducing runoff and sediment transport. Among them, two key concepts were frequently considered in the previous studies (Richet et al., 2014.; Saunier et al., 2018) – the infiltration rate and the hydraulic resistance. The hydraulic resistance is influenced by the frictional forces caused by the litter, stems, or any element present at the soil surface (Gilley and Kottwitz, 1995). The flow velocity is therefore reduced, increasing the depth of the standing water in front of the barrier, diminishing the sediment transport capacity of the water. The presence of vegetation avoids surface crusting and may even increase infiltration by the formation of macroporosity linked to the biological activity and the root system (Kervroëdan et al., 2021) as well as the adds organic matter to the soil, which improves soil structure and water retention.

Table 2. Characteristics of the experimental sites

Vegetative barrier	Years of test	Site	Coordinates (Lambert belge 1972)	Age of plantation during the tests	Soil	Initial planting density	Slope gradient	Vegetation density
	2021	Bruyère (BRU)	X=182379 Y=138129	4 years	Silt- Loam	20000 rhizomes/ha	12%	Plot 1 =48 stems / m ² Plot 2 =43 stems / m ² Plot 3 =58 stems / m ²
	L	Louvain- La-Neuve (LLN1)	X=167973 Y=150368	12 years	Silt- Loam	20000 rhizomes /ha	4%	Plot 1 = 38 stems / m ² Plot 2 = 40 stems / m ² Plot 3 = 35 stems / m ²
	2022	Louvain- La-Neuve (LLN2)	X=169080 Y=150426	7 years	Silt- Loam	20000 rhizomes /ha	5%	Plot 1 =45 stems / m² Plot 2 =40 stems / m² Plot 2 =37 stems / m² Plot 2 =42 stems / m²
Miscanthus giganteus	2023	Mont- Saint- Guibert (MSG)	X=167850 Y=146717	2 years	Silt- Loam	20000 rhizomes /ha	8%	Plot 1 =45 stems /m2 Plot 2 =35 stems / m ² Plot 3 =40 stems / m ² Plot 4 =50 stems / m ²
,		Gembloux (GBX)	X=179747 Y=131760	12 years	Silt- loam	20000 rhizomes/ha	10%	Plot1=52 stems/m2 Plot2=45 stems/m2 Plot3=42 stems/m2 Plot4=60 stems/m2
2024	Ernage (ERN)	X=173738 Y=140997	4 years	Silt- loam	20000 rhizomes/ha	6%	Plot1= 30 stems/m2 Plot2= 43 stems/m2 Plot3= 50 stems/m2 Plot4= 45 stems/m2	
	2022	Genappe (GNP)	X=154359 Y=139319	3 years	Silt- Loam	20000 plants/ ha	4–6%	Plot 1 =6 plants /3 m ² Plot 2=6 plants /3 m ² Plot 3=7 plants /3 m ²
SRC	2023	Eghezée (EGZ)	X=192988 Y=142494	1 year	Silt- Loam	20000 plants/ ha	4–6%	Plot 1 =7 plants /3 m ² Plot 2=6 plants /3 m ² Plot 3 =6 plants /3 m2
	2024	Eghezée (EGZ)	X=192988 Y=142494	2 years	Silt- Loam	20000 plants/ ha	4–6%	Plot 1 =7 plants /3 m ² Plot 1 =7 plants /3 m ² Plot 1 =7 plants /3 m ²

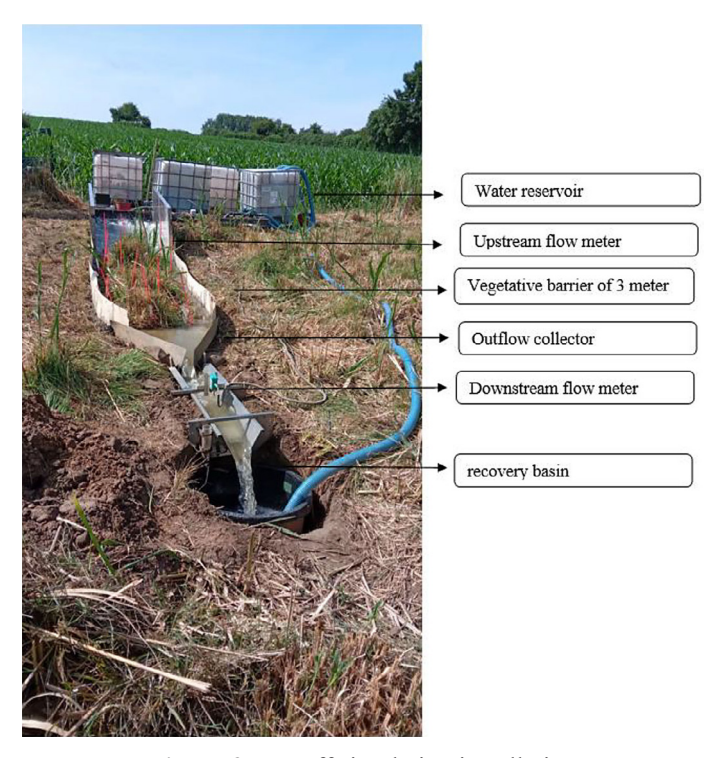


Figure 3. Runoff simulation installation

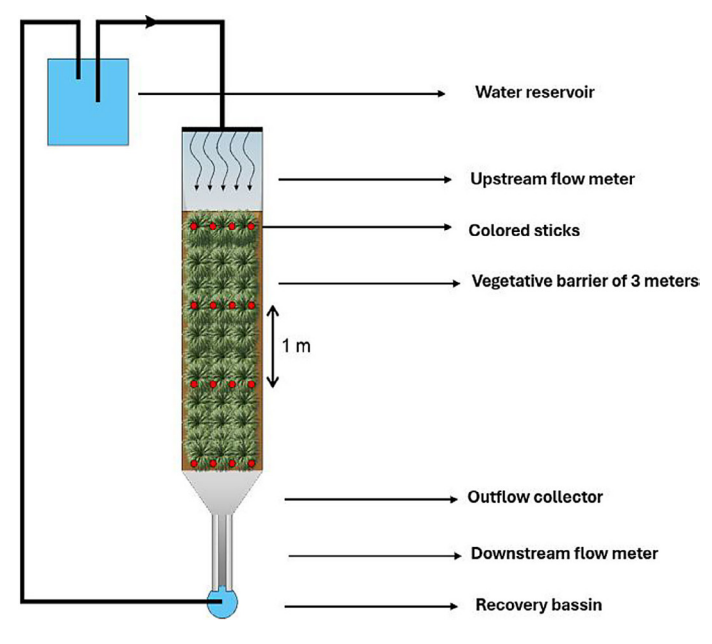


Figure 4. Experimental design

Hydraulic roughness

To determine the hydraulic roughness, we used the empirical Manning coefficient n, consistent with previous studies on vegetative barriers (Bielders et al., 2016; Kervroëdan et al., 2018; Ouvry et al., 2012; Richet et al., 2017). Furthermore, the manning empirical equation is among the most used in models such as SWAT, SWMM,

HEC-RAS, WEPP, and VFSMOD (Richet et al., 2017). Manning coefficient n is defined using:

$$n_m = \frac{A.R^{2/3} \sqrt{S}}{Q} \tag{1}$$

where: n_m – the Manning's resistance coefficient in s.m^{-1/3}, Q – the flow-rate in m³/s; A is the cross-sectional area of flow in square meters m² (to define it we use the formula



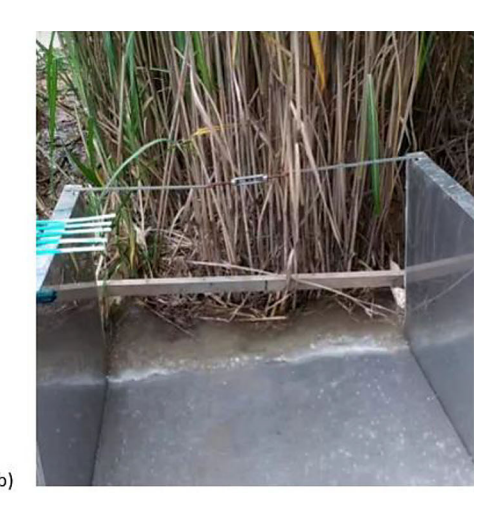


Figure 5. Illustration of colored sticks (a) and simulation of runoff in miscanthus barrier (b)

 $A = L \times h$; where L represents the channel width and h indicates the height of the flow at the vegetation barrier, measured with the colored sticks); R is the hydraulic radius, with R = A/P, P being the wetted perimeter (L + 2h); S is the slope gradient of the vegetation strip in m/m.

It is important to note that water level did not vary significantly within the vegetative barrier. Therefore, to ensure greater accuracy in our study, we integrated the average of the 16 water heights measured across the vegetative strip when computing the Manning coefficient.

Infiltration

During the runoff simulation, a constant inflow was maintained until saturation was achieved. At this point, lateral suction forces were presumed to be negligible, attributing any difference between inflow and outflow solely to vertical infiltration. The calculation of infiltration involved determining the difference in flow rates and dividing it by the undisturbed surface area. This approach allowed for the isolation and quantification of the vertical infiltration process post-saturation.

Statistical analyses of the data

A multiple linear regression analysis was conducted on the acquired data to develop predictive models for the hydraulic roughness of the two tested vegetative barriers based on the field data (age of plantation, slope, density of plantation and flow rate). The accuracy of the resulting models were assessed through k-fold cross-validation (k-fold CV) as outlined by and Benabdelouahab et al.

(2021). K-fold cross-validation serves to evaluate predictive model performance for a specific variable, offering less biased estimates compared to other methods. Unlike sample division validation, which can limit sample size and be influenced by random choices, k-fold CV split the training set into k smaller sets. Models are then constructed using (k-1)/k of data and tested with the remaining 1/k. Our analysis used k = 8 with a repetition number of 8 repeating the k-fold cross-validation process 8 times to ensure robust evaluation of model performance (Benabdelouahab et al., 2021). The N k-fold CV output values were compared with observed values to assess overall model performance. This assessment relied on calculating the root mean square error and correlation coefficient.

RESULTS

Evaluation of the efficiency of *Miscanthus* giganteus and SRC in reducing runoff

Stems densities varied from 30 to 60 stems/m² for *Miscanthus giganteus* depending on the site (Table 3). For SRC, stem density was comprised between 2 and 2.3 stems/m². The hydraulic resistance (Table 3) and the water level (Table 4) was higher for the *Miscanthus giganteus* vegetative barriers compared to the short-rotation coppice (p=0.001). For both vegetation barriers, the Manning coefficient decreased with increasing flow discharge (Figure 6). Moreover, the variability of the Manning coefficient also declined as flow rates increased a phenomenon documented in prior studies (Saunier et al., 2018).

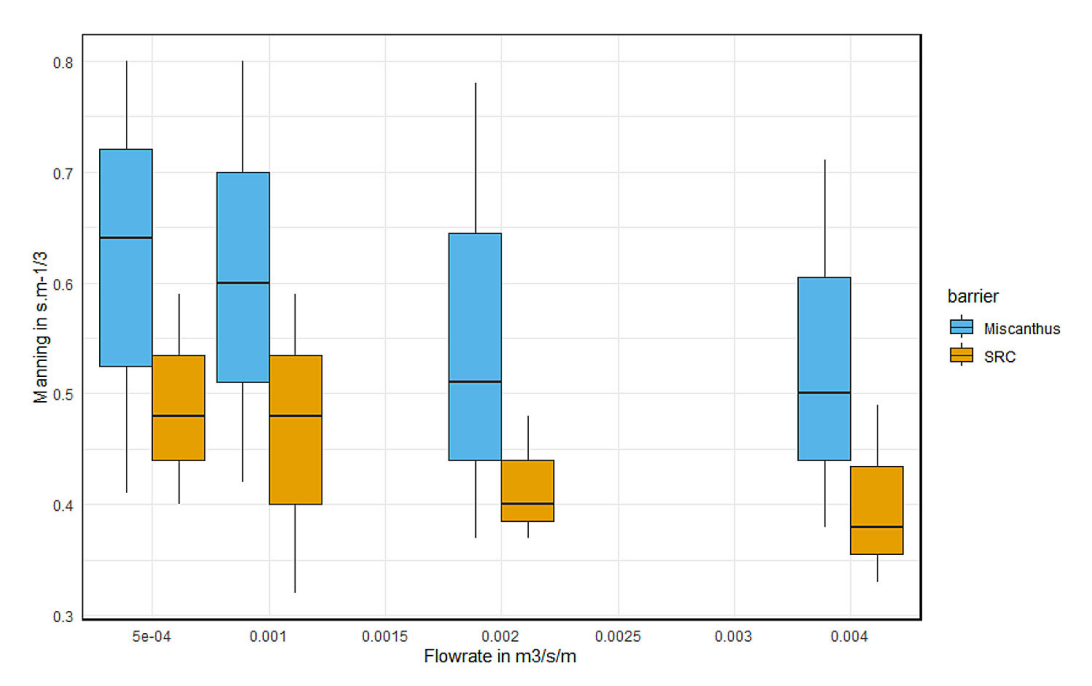


Figure 6. Change in Manning coefficient according to flow rate for the Miscanthus giganteus and SRC barrier

Table 3. Plant or stem d	lensity and Mar	nning coefficient values	s for <i>Miscanthus giganteus</i> and SRC barric	ers
---------------------------------	-----------------	--------------------------	--------------------------------------------------	-----

			0.0
Vegetative barriers Site		Plants or stems density range	Average of Manning coefficient in s.m -1/3
	LLN1	35-40 stems/m ²	0.54±0.13
	LLN2	37–45 stems/m²	0.60±0.17
Missonthus signatous	MSG	35–50 stems/m ²	0.55±0.14
Miscanthus giganteus	BRU	43–58 stems/m ²	0.61±0.14
	ERN	30–50 stems/m ²	0.66±0.04
	GBX	42–60 stems/m ²	0.68±0.01
SRC	GNP	2 to 2.33 plants/m ²	0.41±0.14
	EGZ 2023	2 to 2.33 plants/m ²	0.43±0.12
	EGZ 2024	2 to 2.33 plants/m ²	0.42±0.1

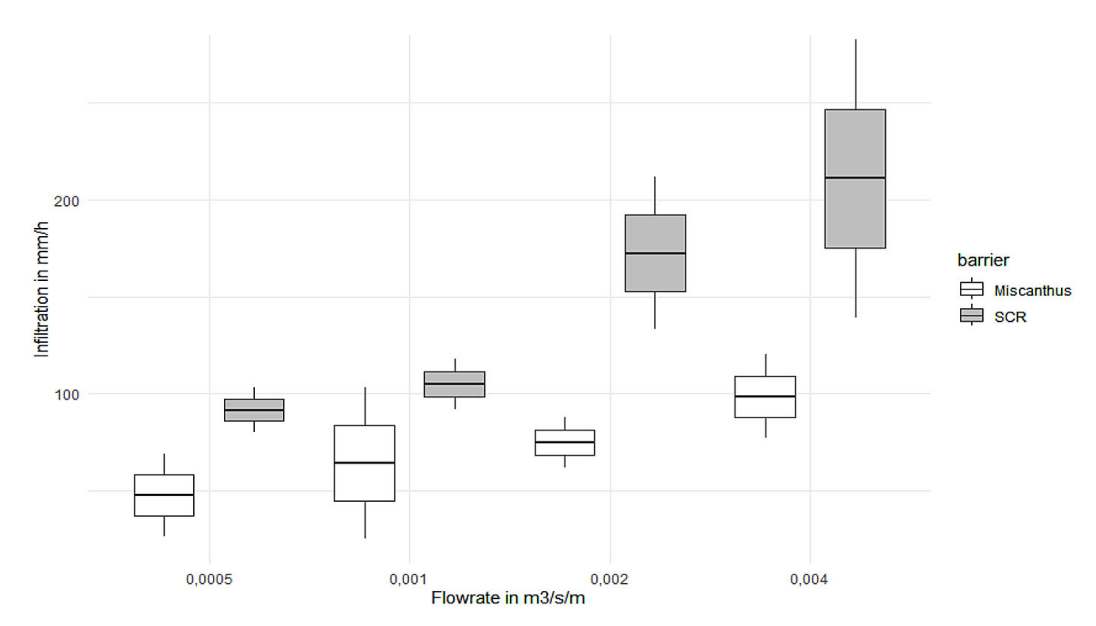


Figure 7. Infiltration rate as function of flow rate for Miscanthus giganteus and SRC barriers

3.30+0.88 cm

2.83+0.80 cm

4.90±1.00 cm

4.80±0.90 cm

	Position from the	Flow rate in m ³ /s					
Parameter	upstream of the vegetation strip	0.0005	0.001	0.002	0.004		
	0.2 m	1.94±0.48 cm	2.50±0.47 cm	3.20±0.03 cm	5.80±1.80 cm		
Miscanthus	1 m	1.98±0.63 cm	2.92±0.79 cm	3.90±0.77 cm	5.10±0.55 cm		
giganteus	2 m	1.89±0.62 cm	2.97±0.46 cm	3.80±0.09 cm	5.90+0.60 cm		
	3 m	2.00±0.09 cm	2.70±0.80 cm	3.50±1.00 cm	4.90±0.90 cm		
	0.2 m	1.50±0.87 cm	2.60±0.66 cm	3.36+1.10 cm	5.20±1.00 cm		
	1 m	2.06±0.80 cm	2.70±1.30 cm	3.80+0.40 cm	5.20±0.80 cm		

2.26±0.41 cm

2.10±1.10 cm

Table 4. Water height in the *Miscanthus giganteus* and SRC vegetative barriers

1.80±1.00 cm

1.40±0.50 cm

Infiltration

SRC

The results reveal that the SRC sites exhibited a superior average infiltration rate of 130 ±30mm/h, compared to the Miscanthus giganteus sites with an average rate of 83±20 mm/h. This underscores the effectiveness of the SRC barriers in facilitating infiltration into the soil. Additionally, Figure 7 illustrates the consistent trend of increased infiltration with higher flow discharges across all studied sites for the four flow rates analyzed. Notably, there is greater variability in infiltration rates observed at higher flow rates.

2 m

3 m

Marginal effect of age of plantation, slope, and density of plantation on hydraulic roughness

To elucidate the variability in Manning coefficient values across experimental conditions, four predictive variables were measured: age of plantation, flow rate, plant or stem density, and the slope gradient of the site. Only the Manning coefficient values measured for flow rates of 0.002 and 0.004 m³/s were used given that the influence of the soil microtopography is least pronounced at these flow rates.

Correlation between variables

For Miscanthus giganteus, we observed robust positive correlations (r = 0.64) between the number of stems per m² and the Manning coefficient. Similarly, for SRC barriers, the correlation coefficient was 0.5 when assessed against density of plots. These correlations highlight a consistently strong positive relationship, implying that an increase in plantation density leads to an increase in the Manning coefficient. Furthermore, for Miscanthus giganteus, a correlation coefficient of 0.3 (Table 5) was identified between hydraulic roughness and slope, indicating a weak relationship between these two variables. However, the analysis for SRC barriers faced limitations due to limited slope variability across the study sites. In terms of flow rate (0.002 and 0.004 m³/s), weak relationships with Manning coefficient values were observed, with correlations of -0.18 and -0.4 for Miscanthus giganteus and SRC, respectively. This observation aligns with the data in Figure 6, indicating that as flow rates increase beyond 0.002 m³/s, the change in hydraulic roughness becomes small. Regarding the age of plantation, the study uncovered correlation coefficients of 0.11 and 0.07 between plantation age and the Manning coefficient for Miscanthus giganteus

Table 5. Simple linear correlations (correlation coefficient) between predictive variables and Manning coefficient

Dominator.	Miscanthus giganteus	SRC	
Parameter Parameter	Manning coefficient	Manning coefficient	
Age	0.11	0.07	
Density of plantation (Nb of stem for <i>Miscanthus giganteus</i> and Nb of plant for SRC)	0.64	0.5	
Slope	0.3	-	
Flow rate	- 0.18	- 0.4	

and SRC barriers, respectively. This implies a weak relationship between the factor and the hydraulic roughness. This is in part attributable to the positive correlation between age and stem density (r = 0.4).

Multiple regression

The studied predictive variables were used to adjust a multiple regression model for the effectiveness of each barrier in limiting runoff (Figure 8). The resulting model demonstrated an R-squared of 0.63 for Miscanthus giganteus and 0.4 for SRC. According to Evans (1996) classification, these values correspond to a strong and

moderate level of conformity, respectively. The adjusted models can be expressed as follows:

Miscanthus giganteus:

Manning coefficient =
$$-0.1 + 1.2 E02 \times A + 0.01 \times Ds + 0.15 \times S - 26.4 \times F$$
 (2)

Short-rotation coppice (SRC):

Manning coefficient =
$$8.9 E - 02 + 0.14 \times Dp + 1.0E - 02 \times A - 16.1 \times F$$
 (3)

where: A – Age of the plantation (years), Ds – Density of plantation (number of stems/ m^2), Dp – Density of plantation (number of plants $/m^2$), S – Slope of the site (m/m), F – Flow rate in m^3/s .

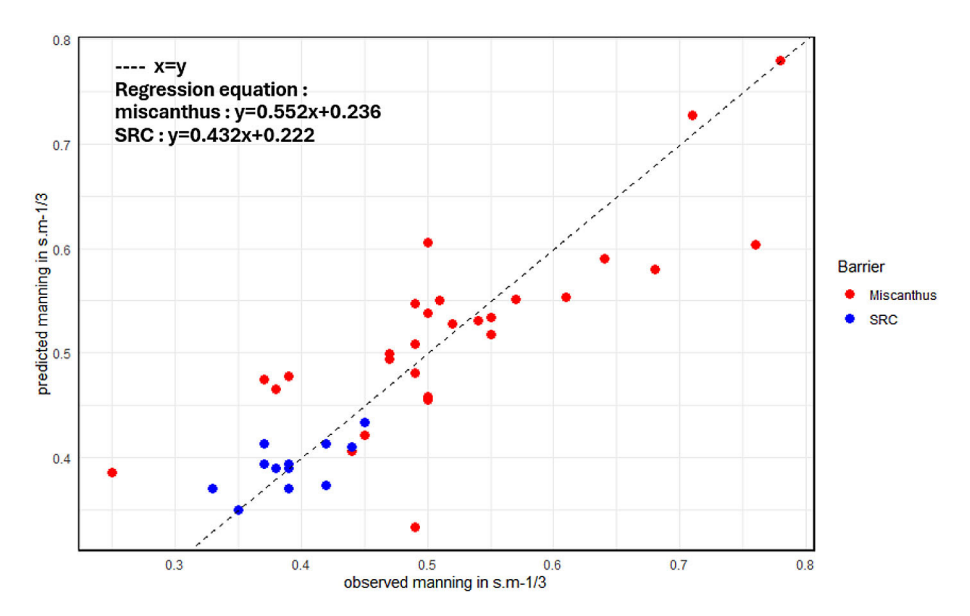


Figure 8. Predicted and observed Manning coefficient for Miscanthus giganteus and SCR barriers

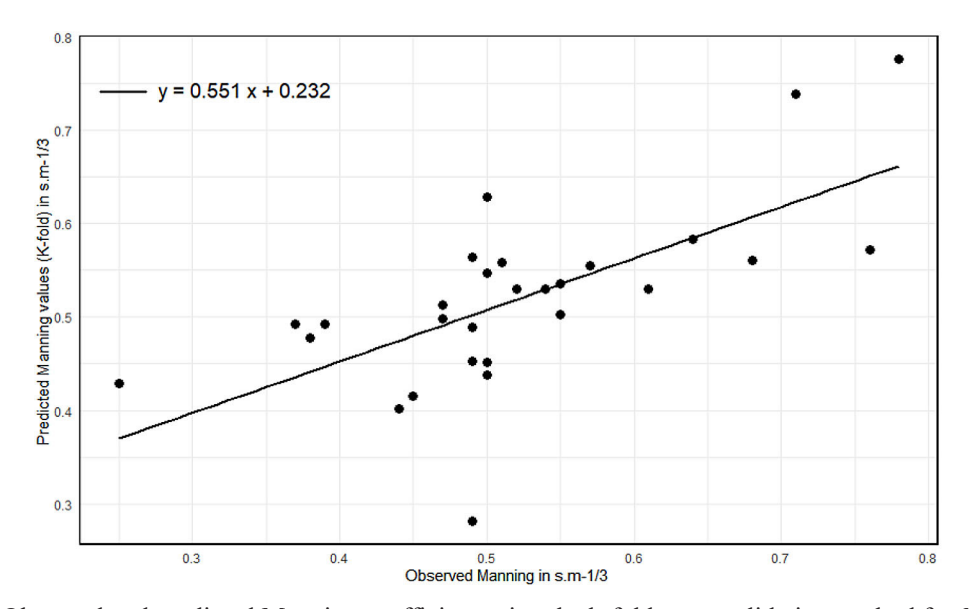


Figure 9. Observed and predicted Manning coefficient using the k-fold cross validation method for *Miscanthus giganteus* barriers

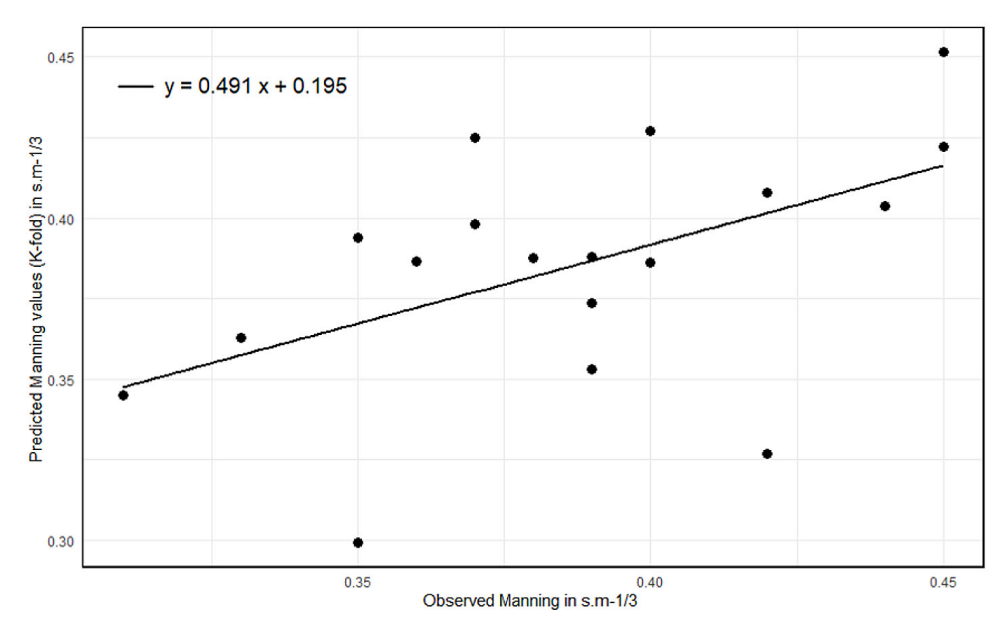


Figure 10. Observed and predicted Manning coefficient using the k-fold cross validation method for SRC barriers

K-fold cross validation

To evaluate the stability of the obtained models for *Miscanthus giganteus* and SRC hydraulic roughness, we compared the Manning coefficient values predicted using an 8-fold CV with those observed in situ (Figure 9 and Figure 10). The statistical indicators derived from this assessment were $R^2 = 0.53$ and RMSE = $0.08 \text{ s.m}^{-1/3}$ which indicate a strong level for *Miscanthus giganteus*. This finding validates the model's capability to accurately estimate the hydraulic roughness of the *Miscanthus giganteus* barrier from the factors studied. However, the model's performance for SRC barriers showed less accuracy with a $R^2 = 0.3$, potentially attributed to the lower number of observations and a more limited range of n values.

DISCUSSION

The barriers studied demonstrated significant effectiveness in restricting runoff flow, with Manning's roughness coefficients ranging from 0.37 to 0.8 s.m^{-1/3} for *Miscanthus giganteus* and 0.32 to 0.59 s.m^{-1/3} for SRC. These findings align with previous research, which reported Manning coefficient values of 0.4 to 0.7 s.m^{-1/3} for *Miscanthus giganteus* and 0.30 to 0.50 s.m^{-1/3} for SRC (Richet et al., 2019; Saunier et al., 2018). However, our results highlight the influence of multiple site-dependent factors on hydraulic resistance.

For both types of vegetative barriers, the hydraulic roughness exhibits a decrease with increasing flow discharge. This finding aligns with existing literature (Richet et al., 2017; Saunier et al., 2018). At lower discharges, roughness is more strongly influenced by microtopographic variation and surface litter than at higher discharge rates. Variability across sites was more pronounced in Miscanthus giganteus plots, where factors such as stem density, slope gradient, and plantation age had noticeable effects. Our study revealed that slope has a moderately positive impact on hydraulic roughness in Miscanthus giganteus barriers, with a correlation coefficient value of 0.3 likely due to a decrease in water depth at constant discharge, which enhances the contribution of microtopography and surface mulch. In contrast, slope variation was minimal in the SRC plots, limiting the ability to assess its impact on Manning's coefficient. Additionally, the impact of plantation age on hydraulic roughness was less significant, most likely due to the relatively uniform age of SRC sites and the mature stage (over three years) of most Miscanthus giganteus barriers tested, except for the MSG site. Previous studies (Miguez et al., 2008; Ouattara et al., 2020) indicate that Miscanthus giganteus biomass stabilizes after three years, with differences primarily in stem distribution rather than total biomass.

Stem density emerged as a crucial factor in determining hydraulic roughness. A regression model indicated a strong correlation (r=0.64)

between *Miscanthus giganteus* stem density and hydraulic roughness, while a moderate correlation (r=0.5) was found for SRC barriers. Prior studies (Mekonnen et al., 2016; Morgan and Duzant, 2008) support the role of plant density in regulating flow velocity and erosion. However, Kervroëdan et al., 2018 suggested that the stem density of herbaceous hedges does not influence hydraulic roughness, possibly due to inherent differences in morphological traits among vegetative barriers.

The lower R2 values for SRC and the moderate R² for Miscanthus giganteus in our models may be attributed to the influence of additional factors not included in the regression analysis. One such factor is the presence of mulch, which has been shown to significantly affect Miscanthus giganteus hydraulic roughness by increasing surface resistance and altering flow pathways, thereby reducing flow velocity and enhancing water retention (Richet et al., 2014). Similarly, grass cover within SRC barriers has been found to impact Manning's coefficient (Saunier et al., 2018). The omission of these variables from our analysis may explain the observed variability in model performance. Future research incorporating standardized measurements of these factors could improve model accuracy and provide deeper insights into the hydraulic behavior of vegetative barriers.

SRC barriers demonstrated superior water infiltration capacity compared to Miscanthus giganteus. Our study recorded infiltration rates of 83±20 mm/h for Miscanthus giganteus and 130±30 mm/h for SRC. These findings align with previous studies reporting Miscanthus giganteus infiltration rates between 20 and 131 mm/h in sandy loamy soils (Richet et al., 2014; Saunier et al., 2018) and SRC infiltration rates ranging from 60 to 100 mm/h in loamy soils (Saunier et al., 2018). However, these rates remain lower than those observed in other vegetative barriers, such as shrub hedges (Richet et al., 2017) and grass hedges (Rachman et al., 2004). SRC's superior infiltration capacity is attributed to its extensive, fibrous root system, which enhances soil porosity and water movement (Langeveld et al., 2012). In contrast, while Miscanthus giganteus possesses a deep root system, its growth pattern may limit soil pore space development, potentially reducing infiltration efficiency.

Our analysis also revealed that infiltration rates increased with higher flow rates, consistent with the findings of (Richet et al., 2017). This trend can likely be attributed to the greater

hydrostatic pressure exerted by deeper water layers, which enhances infiltration. However, as noted by (Richet et al., 2017), the limited surface area of the runoff simulator resulted in a negligible volume of infiltrated water relative to total inflow. This experimental constraint introduced significant uncertainty in the calculated infiltration rates.

Overall, our findings confirm that both *Miscanthus giganteus* and SRC vegetative barriers effectively mitigate runoff impacts on soil. The density of *Miscanthus giganteus* stems per m² and the number of SRC plants per m² in the runoff axis are critical factors influencing their efficiency. Land managers should consider these parameters when implementing vegetative barriers to maximize their effectiveness in soil and water conservation.

CONCLUSIONS

The vegetative barriers investigated in this research exhibit significant advantages in slowing down runoff and enhancing soil infiltration. The developed model serves as a valuable tool for simulating the effectiveness of these vegetative barriers under varying site conditions. By integrating key factors, the model enables a comprehensive understanding of how these barriers perform in different environmental settings. This simulation capability not only enhances our grasp of the barriers' effectiveness but also provides practical insights for optimizing their performance based on specific site conditions. In essence, the model contributes to a more nuanced and adaptable approach to implementing vegetative barriers, ensuring their efficacy across diverse landscapes and scenarios.

In addition to their crucial role in mitigating surface runoff and soil erosion, both Miscanthus x giganteus and short-rotation coppice (SRC) barriers offer substantial economic benefits through biomass production beyond their hydraulic properties. Miscanthus is a promising perennial bioenergy crop in Europe as well as a feedstock for biobased materials. Its biomass also finds application as animal bedding and agricultural mulch. Similarly, SRC systems, typically involving willow or poplar, generate significant amounts of woody biomass on short cycles (3–5 years). This biomass can be mechanically harvested and utilized as a renewable energy feedstock or as a raw material for the pulp and paper industry. The inherent

multifunctionality of these crops positions them as attractive options for sustainable land management strategies. Other similarly multifunctional crops would deserve hydraulic properties quantification such as the one presented here.

However, it is essential to note that certain factors, such as soil characteristics, mulch density in *Miscanthus giganteus* barriers and the type of grass in SRC barriers, have not been considered in our study. Furthermore, exploring a wider range of plant densities, slope gradients, and age of the plantation is necessary to validate the models developed in our study for both Miscanthus giganteus and SRC vegetative barrier. Recognizing these omissions encourages further investigation to attain a more comprehensive and accurate understanding of the dynamics at play. Future research endeavors should explore the influence of mulch density and specific grass types on the performance of vegetative barriers, contributing to a more nuanced and refined model.

Acknowledgements

This study was supported by the Service Public de Wallonie through the financing of the Intell'eau projects. We also thank the CIPF engineers and technicians for their implementation and support at the experimental sites.

REFERENCES

- Aboutayeb, R., El Yousfi, B., El Gharras, O., (2020). Impact of No-Till on physicochemical properties of Vertisols in Chaouia region of Morocco. *EUR-ASIAN J. SOIL Sci. EJSS 9*, 119–125. https://doi. org/10.18393/ejss.663502
- 2. Benabdelouahab, T., Lebrini, Y., Boudhar, A., Hadria, R., Htitiou, A., Lionboui, H., (2021). Monitoring spatial variability and trends of wheat grain yield over the main cereal regions in Morocco: a remote-based tool for planning and adjusting policies. *Geocarto Int.* 36, 2303–2322. https://doi.org/10.1080/10106049.2019.1695960
- 3. Bielders, C., Degré, A., Demarcin, P., de Walque, Baptiste, Dewez, A., Pineux, N., Staquet, J.-B., Swerts, G., (2016). Giser: Gestion intégrée sol-érosion-ruissellement Rapport d'activités 2015–2016.
- 4. Bissonnais, Y.L., Thorette, J., Bardet, C., Daroussin, J., n.d. L'EROSION HYDRIQUE DES SOLS EN FRANCE.
- Blanco-Canqui, H., Gantzer, C.J., Anderson, S.H., Alberts, E.E., Thompson, A.L., (2004). Grass barrier

- and vegetative filter strip effectiveness in reducing runoff, sediment, nitrogen, and phosphorus loss. *Soil Sci. Soc. Am. J. 68*, 1670–1678. https://doi.org/10.2136/sssaj2004.1670
- Dabney, S.M., Wilson, G.V., McGregor, K.C., Vieira, D.A.N., 2012. Runoff through and upslope of contour switchgrass hedges. *Soil Sci. Soc. Am. J.* 76, 210–219. https://doi.org/10.2136/sssaj2011.0019
- 7. Eppler, U., Petersen, J.-E., 2007. Short Rotation Forestry, Short Rotation Coppice and energy grasses in the European Union: Agro-environmental aspects, present use and perspectives.
- 8. Evans, J.D. (1996). *Straightforward Statistics* for the Behavioral Sciences. Pacific Grove, CA: Brooks/Cole Publishing Co.
- Evers, B.J., Blanco-Canqui, H., Staggenborg, S.A., Tatarko, J., (2013). Dedicated bioenergy crop impacts on soil wind erodibility and organic carbon in Kansas. *Agron. J.* 105, 1271–1276. https://doi.org/10.2134/agronj2013.0072
- 10. Frankl, A., De Boever, M., Bodyn, J., Buysens, S., Rosseel, L., Deprez, S., Bielders, C., Dégre, A., Stokes, A., (2021). Report on the effectiveness of vegetative barriers to regulate simulated fluxes of runoff and sediment in open agricultural landscapes (Flanders, Belgium). *Land Degrad. Dev.* 32, 4445– 4449. https://doi.org/10.1002/ldr.4048
- Freeman, G.E., Rahmeyer, W.H., Copeland, R.R., (2000). Determination of Resistance Due to Shrubs and Woody Vegetation: Defense Technical Information Center, Fort Belvoir, VA. https://doi. org/10.21236/ADA383997
- 12. Gao, Y., Zhu, B., Zhou, P., Tang, J.-L., Wang, T., Miao, C.-Y., (2009). Effects of vegetation cover on phosphorus loss from a hillslope cropland of purple soil under simulated rainfall: a case study in China. *Nutr. Cycl. Agroecosystems* 85, 263–273. https://doi.org/10.1007/s10705-009-9265-8
- 13. Gobin, A., Govers, G., Jones, R., (2003). Assessment and reporting on soil erosion: background and workshop report. EEA, Copenhagen.
- 14. Gyssels, G., Poesen, J., Bochet, E., Li, Y., (2005). Impact of plant roots on the resistance of soils to erosion by water: a review. *Prog. Phys. Geogr. Earth Environ.* 29, 189–217. https://doi.org/10.1191/0309133305pp443ra
- 15. Heaton, E.A., Dohleman, F.G., Long, S.P., (2008). Meeting US biofuel goals with less land: the potential of Miscanthus. Glob. Change Biol. 14, 2000–2014. https://doi.org/10.1111/j.1365-2486.2008.01662.x
- Herpoel, M., Bielders, C., Baert, P., Michez, A., Meersmans, J., Degré, A., (2025). Field patterns as game changers of the sediment connectivity. *Geo-morphology* 477, 109679. https://doi.org/10.1016/j. geomorph.2025.109679

- 17. J. E. Gilley, E. R. Kottwitz, (1995). Darcy-weisbach roughness coefficients for surfaces with residue and gravel cover. *Trans. ASAE 38*, 539–544. https://doi.org/10.13031/2013.27863
- 18. Kahle, P., Janssen, M., (2020). Impact of short-rotation coppice with poplar and willow on soil physical properties. *J. Plant Nutr. Soil Sci. 183*, 119–128. https://doi.org/10.1002/jpln.201900443
- Kervroëdan, L., Armand, R., Rey, F., Faucon, M., (2021). Trait-based sediment retention and runoff control by herbaceous vegetation in agricultural catchments: A review. *Land Degrad. Dev.* 32, 1077– 1089. https://doi.org/10.1002/ldr.3812
- Kervroëdan, L., Armand, R., Saunier, M., Ouvry, J.-F., Faucon, M.-P., (2018). Plant functional trait effects on runoff to design herbaceous hedges for soil erosion control. *Ecol. Eng. 118*, 143–151. https://doi.org/10.1016/j.ecoleng.2018.04.024
- 21. Langeveld, H., Quist-Wessel, F., Dimitriou, I., Aronsson, P., Baum, C., Schulz, U., Bolte, A., Baum, S., Köhn, J., Weih, M., Gruss, H., Leinweber, P., Lamersdorf, N., Schmidt-Walter, P., Berndes, G., (2012). Assessing environmental impacts of short rotation coppice (SRC) expansion: Model definition and preliminary results. *BioEnergy Res.* 5, 621–635. https://doi.org/10.1007/s12155-012-9235-x
- 22. Lewin, E., Kiesel, A., Magenau, E., Lewandowski, I., (2023). Integrating perennial biomass crops into crop rotations: How to remove miscanthus and switchgrass without glyphosate. *GCB Bioenergy 15*, 1387–1404. https://doi.org/10.1111/gcbb.13099
- 23. Mekonnen, M., Keesstra, S.D., Ritsema, C.J., Stroosnijder, L., Baartman, J.E.M., (2016). Sediment trapping with indigenous grass species showing differences in plant traits in northwest Ethiopia. *CATENA 147*, 755–763. https://doi.org/10.1016/j. catena.2016.08.036
- 24. Miguez, F.E., Villamil, M.B., Long, S.P., Bollero, G.A., (2008). Meta-analysis of the effects of management factors on Miscanthus×giganteus growth and biomass production. *Agric. For. Meteorol.* 148, 1280–1292. https://doi.org/10.1016/j.agrformet.2008.03.010
- 25. Morgan, R.P.C., Duzant, J.H., (2008). Modified MMF (Morgan–Morgan–Finney) model for evaluating effects of crops and vegetation cover on soil erosion. *Earth Surf. Process. Landf.* 33, 90–106. https://doi.org/10.1002/esp.1530
- 26. Ouattara, M.S., Laurent, A., Barbu, C., Berthou, M., Borujerdi, E., Butier, A., Malvoisin, P., Romelot, D., Loyce, C., (2020). Effects of several establishment modes of *Miscanthus* × *giganteus* and *Miscanthus sinensis* on yields and yield trends. *GCB Bioenergy* 12, 524–538. https://doi.org/10.1111/gcbb.12692
- 27. Ouvry, J., Richet, J., Bricard, O., LHÉRITEAU, M.,

- Bouzid, M., Saunier, M., (2012). Fascines & haies pour réduire les effets du ruissellement érosif Caractérisation de l'efficacité et conditions d'utilisation.
- Pan, D., Gao, X., Dyck, M., Song, Y., Wu, P., Zhao, X., (2017). Dynamics of runoff and sediment trapping performance of vegetative filter strips: Run-on experiments and modeling. *Sci. Total Environ.* 593–594, 54–64. https://doi.org/10.1016/j.scitotenv.2017.03.158
- Pimentel, D., Harvey, C., Resosudarmo, P., Sinclair, K., Kurz, D., McNair, M., Crist, S., Shpritz, L., Fitton, L., Saffouri, R., Blair, R., (1995). Environmental and economic costs of soil erosion and conservation benefits. *Science* 267, 1117–1123. https://doi.org/10.1126/science.267.5201.1117
- 30. Rachman, A., Anderson, S.H., Gantzer, C.J., Alberts, E.E., (2004). Soil Hydraulic properties influenced by stiff-stemmed grass hedge systems. *Soil Sci. Soc. Am. J. 68*, 1386–1393. https://doi.org/10.2136/sssaj2004.1386
- 31. Richet, J., Kervroëdan, L., Saunier, M., Ouvry, J., (2019). La haie herbacée antiérosive, une zone tampon efficace pour la rétention des particules.
- 32. Richet, J.-B., Gril, J.-J., Ouvry, J.-F., n.d. Infiltrabilité de dispositifs enherbés du Pays de Caux, premiers résultats.
- 33. Richet, J.-B., Ouvry, J.-F., Saunier, M., (2017). The role of vegetative barriers such as fascines and dense shrub hedges in catchment management to reduce runoff and erosion effects: Experimental evidence of efficiency, and conditions of use. *Ecol. Eng.* 103, 455–469. https://doi.org/10.1016/j.ecoleng.2016.08.008
- 34. Rodrigues, A.R., Marques, S., Botequim, B., Marto, M., Borges, J.G., (2021). Forest management for optimizing soil protection: a landscape-level approach. *For. Ecosyst.* 8, 50. https://doi.org/10.1186/s40663-021-00324-w
- 35. Salles, C., Poesen, J., Govers, G., (2000). Statistical and physical analysis of soil detachment by raindrop impact: Rain erosivity indices and threshold energy. *Water Resour. Res.* 36, 2721–2729. https:// doi.org/10.1029/2000WR900024
- 36. Saunier, M., Ouvry, J., Verger, A., (2018). Rapport «INNOBIOMA programme de recherche sur les bandes ligno-cellulosiques capacités d'infiltration et de sédimentation sous saules (TTCR) et sous miscanthus », Saunier et al. (AREAS), 2018.
- 37. Souiller, C., Coquet, Y., Pot, V., Benoit, P., Réal, B., Margoum, C., Laillet, B., Labat, C., Vachier, P., (2002). Capacités de stockage et d'épuration des sols de dispositifs enherbés vis-à-vis des produits phytosanitaires. Étude Gest. Sols.
- 38. Urrego, J.P.F., Huang, B., Næss, J.S., Hu, X., Cherubini, F., (2021). Meta-analysis of leaf area index, canopy height and root depth of three bioenergy crops and their effects on land surface modeling.

- *Agric. For. Meteorol.* 306, 108444. https://doi.org/10.1016/j.agrformet.2021.108444
- 39. Van Dijk, P.M., Kwaad, F.J.P.M., Klapwijk, M., (1996). Retention of water and sediment by grass strips. *Hydrol. Process.* 10, 1069–1080. https://doi.org/10.1002/(SICI)1099-1085(199608)10:8<1069::AID-HYP412>3.0.CO;2-4
- Wallace, E.E., McShane, G., Tych, W., Kretzschmar, A., McCann, T., Chappell, N.A., (2021). The effect of hedgerow wild-margins on topsoil hydraulic properties, and overland-flow incidence, magnitude and water-quality. *Hydrol. Process.* 35, e14098. https://doi.org/10.1002/hyp.14098
- 41. Xiong, K., Yin, C., Ji, H., (2018). Soil erosion and chemical weathering in a region with typical karst topography. *Environ. Earth Sci.* 77, 500. https://doi.org/10.1007/s12665-018-7675-0
- 42. Yuan, Y., Bingner, R.L., Locke, M.A., (2009). A

- Review of effectiveness of vegetative buffers on sediment trapping in agricultural areas. *Ecohydrology* 2, 321–336. https://doi.org/10.1002/eco.82
- 43. Zhang, L., Wang, J., Bai, Z., Lv, C., (2015). Effects of vegetation on runoff and soil erosion on reclaimed land in an opencast coal-mine dump in a loess area. *CATENA 128*, 44–53. https://doi.org/10.1016/j.catena.2015.01.016
- 44. Zhao, C., Nie, Y., Xin, J., Zhu, X., Li, Y., Tian, R., (2023). Soil erosion effectively alleviated by Miscanthus sacchariflorus, a potential candidate for land deterioration improvement. *Rhizosphere 26*, 100694. https://doi.org/10.1016/j.rhisph.2023.100694
- 45. Zub, H.W., Brancourt-Hulmel, M., (2010). Agronomic and physiological performances of different species of Miscanthus, a major energy crop. A review. *Agron. Sustain. Dev.* 30, 201–214. https://doi.org/10.1051/agro/2009034